



**HAL**  
open science

# Influence of zirconium on the structure of pristine and leached soda-lime borosilicate glasses: Towards a quantitative approach by $^{17}\text{O}$ MQMAS NMR

Frédéric Angeli, Thibault Charpentier, Marina Gaillard, Patrick Jollivet

## ► To cite this version:

Frédéric Angeli, Thibault Charpentier, Marina Gaillard, Patrick Jollivet. Influence of zirconium on the structure of pristine and leached soda-lime borosilicate glasses: Towards a quantitative approach by  $^{17}\text{O}$  MQMAS NMR. *Journal of Non-Crystalline Solids*, 2008, 354 (31), pp.3713-3722. 10.1016/j.jnoncrysol.2008.03.046 . cea-02512525

**HAL Id: cea-02512525**

**<https://cea.hal.science/cea-02512525>**

Submitted on 19 Mar 2020

**HAL** is a multi-disciplinary open access archive for the deposit and dissemination of scientific research documents, whether they are published or not. The documents may come from teaching and research institutions in France or abroad, or from public or private research centers.

L'archive ouverte pluridisciplinaire **HAL**, est destinée au dépôt et à la diffusion de documents scientifiques de niveau recherche, publiés ou non, émanant des établissements d'enseignement et de recherche français ou étrangers, des laboratoires publics ou privés.

# **$^{17}\text{O}$ and $^{11}\text{B}$ NMR Investigation of the Effect of Zirconium on the Structure of Soda-Lime Borosilicate Glass and its Alteration Layer**

Frédéric Angeli<sup>1</sup>, Marina Gaillard<sup>2</sup>, Thibault Charpentier<sup>2</sup>, Patrick Jollivet<sup>1</sup>

<sup>1</sup>*Laboratoire d'Étude du Comportement à Long Terme,  
DEN/DTCD/SECM, CEA Valrhô, 30207 Bagnols-sur-Cèze Cedex, France*

<sup>2</sup>*Laboratoire de Structure et Dynamique par Résonance Magnétique,  
DSM/DRECAM/SCM, CEA Saclay, 91191 Gif-sur-Yvette Cedex, France*

## **Abstract**

$^{17}\text{O}$  MAS, MQMAS NMR and  $^{11}\text{B}$  MAS NMR were used to obtain data on the structure of soda-lime borosilicate glass containing zirconium. A method of quantitative analysis of the  $^{17}\text{O}$  MQMAS spectra is presented, by fitting directly the two-dimensional MQMAS spectrum which provides the resolution of all the structural groups forming the glass network. Additional data for this analysis are also obtained from the quantitative deconvolution of the  $^{11}\text{B}$  MAS NMR spectra. Similar compositions but without oxygen-17 enrichment were altered in a solution of water enriched in oxygen-17. Preferential compensation mechanisms of sodium with respect to boron and zirconium rather than calcium in the glass are proposed. Although most of the zirconium is inserted in the silicate network forming Si-O-Zr bonds, the presence of this element tends to reduce the extent of a borate subnetwork by forming B-O-Zr bonds. Excess nonbridging oxygen is clearly identified in the glasses, and could be related to the presence of oxygen triclusters. During leaching, calcium clearly remains in the alteration gel, either stabilized near nonbridging oxygens or as a zirconium charge compensator, as zirconium conserves the same coordination number than in the glass. Zirconium increases the rigidity of the glass structure by making silicon dissolution and reprecipitation more difficult, resulting in larger quantities of altered glass.

PACS: 61.43.Fs; 76.60.-k

## 1. Introduction

The alteration layer (commonly known as the “gel”) that forms during the alteration of borosilicate glasses by water account for a drop in the glass alteration rate and can develop retention properties with respect to some vitreous matrix constituent elements [1]. These properties could be significantly influenced by the gel structure itself. During leaching, rearrangements among structural groups are related to the pristine glass chemical composition and could also depend in part on the initial glass structure [2]. Structural characterization of the gel according to the glass composition can thus be useful for a better understanding of the alteration mechanisms. These issues affect many areas for which the reactivity of the glass must be known: conditioning glass, archaeological glass, or radioactive waste containment glass repositories.

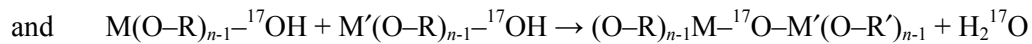
As being bonded to both network formers and modifiers, the oxygen atom is an ideal probe of the structure of oxide glasses, after oxygen-17 isotopic enrichment. However the standard sample magic-angle spinning (MAS) technique cannot resolve the different oxygen sites when the glass contains several oxides. The overlap between different sites on one-dimensional spectra generally requires the use of two-dimensional experiments, such as the MQMAS experiment [3]. It has been applied to glasses containing up to four oxides, mainly borates, borosilicates, aluminosilicates and aluminoborosilicate containing alkalis or alkaline earths, and in which bridging and nonbridging oxygen groups were identified [4–10]. We also demonstrated for the first time a few years ago its strong potential for characterizing the structural groups forming the gel [11]. The reconstruction of an aluminosilicate gel with the same structural configuration as the pristine glass but without nonbridging oxygens (NBO) was pointed out during leaching.

In this paper we first highlight the possibility of resolving all the structural groups in a glass containing up to five oxides. The combined use of experimental data  $^{11}\text{B}$  and  $^{17}\text{O}$  NMR and structural models may inform about possible synergies between charge compensators and network formers. No experimental methods available today are capable of directly determining the nature of the cation near a network former when there is competition between different types of charge compensators (e.g. alkalis and alkaline earths). In the present work, we are especially focusing on two types of elements requiring charge compensation: four-coordinate boron and six-coordinate zirconium. In the second part of this study, similar compositions but without oxygen-17 enrichment were altered in a solution of water enriched in

oxygen-17. Directly characterizing the exchange sites between the solution and the glass provides selective data on the gel structure, which can then be related to the pristine glass structure. Two glass compositions with the major elements of waste containment glass were investigated: one comprising four oxides ( $70\text{SiO}_2-17.8\text{B}_2\text{O}_3-9.9\text{Na}_2\text{O}-2.3\text{CaO}$ ) and a second also containing zirconium ( $67.2\text{SiO}_2-15.5\text{B}_2\text{O}_3-10.4\text{Na}_2\text{O}-3.3\text{CaO}-3.6\text{ZrO}_2$ ). Zirconium has a major effect on the gel structure and glass reactivity [12]. The same type of composition, but richer in alkalis to obtain a larger quantity of gel, was then altered in  $\text{H}_2^{17}\text{O}$  to study the structure of the alteration gel formed on unenriched pristine glass. The distribution of alkalis and alkaline earths in the glass structure and in the gel is another item of interest in this type of composition. Examining changes between network-modifying and charge-compensating positions can lead to a better understanding of the leaching mechanisms [2].

## 2. Experimental conditions

**Fabrication of glass enriched in oxygen-17.** The materials were synthesized by the sol-gel process, involving hydrolysis (70% enriched water) and polycondensation from metal alkoxides in an organic medium. The metal precursors used for glass fabrication were enriched according to the following reactions:



where: M and M' are cations; R and R' are organic groups

The advantage of this method is that it can enrich all the glass precursors in oxygen-17. The resulting precursors were melted for 15 minutes on platinum foil at  $1220^\circ\text{C}$ . The glass was analyzed by alkaline fusion ( $\text{NaOH}+\text{KNO}_3$  and  $\text{Li}_2\text{B}_4\text{O}_7, 5\text{H}_2\text{O}$ ) of powder samples ( $\sim 50$  mg) then dissolved in  $\text{HNO}_3$  for ICP-AES analysis. A paramagnetic element ( $\text{Gd}_2\text{O}_3$ ) was added to the glass in very small quantities (0.2 wt%) to diminish the relaxation time of the  $^{17}\text{O}$  nucleus during NMR spectrum acquisition without modifying the glass structure.

**Glass leaching.** The glass without oxygen-17 enrichment was leached in contact with water enriched in oxygen-17. The glass specimens were ground in tungsten carbide bowls then screened to recover the

particle size fraction between 125 and 250  $\mu\text{m}$ . The powder was washed in acetone to eliminate the fine glass particles. The specific surface area of this particle size fraction measured by krypton adsorption using the BET method was  $380 \text{ cm}^2 \cdot \text{g}^{-1}$ . Glass specimens were leached in static mode, unstirred, at  $90^\circ\text{C}$  in water enriched to 47% for the glass without zirconium and 70% for the glass containing zirconium, for 176 days with a glass-Surface-Area-to-solution-Volume ratio (SA/V) of  $120 \text{ cm}^{-1}$ . The enrichment was higher in the second case because oxygen atoms near Zr are theoretically more difficult to exchange with oxygen-17.

**MAS and MQMAS NMR.** All the spectra were collected on a Avance Bruker 500WB spectrometer (magnetic field 11.74 T), using a Bruker 4 mm (o.d.) CPMAS probe at a spin frequency ranging from 12.5 kHz to 14 kHz. For  $^{11}\text{B}$  ( $I = 3/2$ ,  $\nu_0 = 160.14 \text{ MHz}$ ), simple acquisition spectra were obtained with repetition times of 1 s using short (1  $\mu\text{s}$ ) pulses to obtain a quantitative spectrum (nuclei with spins greater than  $1/2$  are subjected to quadrupolar interaction that interferes with the radiofrequency field during the excitation pulse, resulting in a non-quantitative spectrum except with very short pulses corresponding to linear conditions [13]. The chemical shift is referenced to a 1 M (19.6 ppm) boric acid solution. Concerning  $^{17}\text{O}$  ( $I = 5/2$ ,  $\nu_0 = 67.67 \text{ MHz}$ ), MAS and MQMAS spectra were acquired with a sample rotation speed of 14 kHz, a 71.5  $\mu\text{s}$  increment in the first dimension (64 points along the first dimension  $t_1$ , synchronized with the rotation), and a 1 s repetition time (4500 FIDs for each  $t_1$  value). We used a Z-filter sequence with first and second pulse durations of 7  $\mu\text{s}$  and 2.6  $\mu\text{s}$  (RF field estimated at 60 kHz), and a third 5.5  $\mu\text{s}$  pulse  $\pi/2$  selective on the central transition (RF field: 15 kHz) [14]. The spectra were analyzed (fitting, simulation and inversion) with an homebuilt software, using a theoretical approach described in [15]. It should be pointed out that the dependence upon the NMR parameters (mainly the quadrupolar coupling constant) of the efficiency of the MQMAS pulse sequence was taken into account in order to devise a quantitative analysis of the MQMAS data. This was explained in [16], as well as the principles of modeling the MQMAS spectrum of amorphous systems. Details are given below.

### 3. Results and discussion

#### 3.1 Glass structure

Two glass compositions were enriched in oxygen-17: a borosilicate containing sodium and calcium (designated  $^{17}\text{O-Si}$ ) and another also containing zirconium (designated  $^{17}\text{O-Si-Zr}$ ) (**Table I**).

$^{11}\text{B}$  MAS NMR is traditionally used to quantify the proportion of three-coordinate ( $\text{BO}_3$ ) and four-coordinate ( $[\text{BO}_4]^-$ ) species. The  $^{11}\text{B}$  MAS spectra of glass samples enriched in oxygen-17 are superimposed in **Figure 1** with the simulated spectra used to quantify the sites. Four-coordinate boron corresponds to the site with the lowest quadrupolar coupling (the narrowest peak). Quantifying the sites clearly shows that adding zirconium to the glass results in a very significant drop in the number of four-coordinate boron atoms (**Table II**).

The Dell & Bray model established for ternary borosilicate glass [17–19] estimates the proportions of three-coordinate ( $N_3$ ) and four-coordinate ( $N_4$ ) boron according to the chemical composition assuming the existence of particular borosilicate units (diborates, reedmergnerites, etc.). The model is based on the  $R = \text{Na}_2\text{O}/\text{B}_2\text{O}_3$  and  $K = \text{SiO}_2/\text{B}_2\text{O}_3$  molar ratios. In borosilicates the number of  $N_4$  increases proportionally with the total number of alkalis up to a maximum value (for  $R = 1$ ) above which it stabilizes and then linearly diminishes as the sodium fraction increases. When network formers requiring charge compensation are added (such as  $[\text{AlO}_4]^-$  groups), the number of  $N_4$  then becomes proportional to the number of alkalis still available after compensating the aluminum [20,21]. Nevertheless, the degree of mixing between boron and silicon is generally greater than predicted by the model for this type of composition [11]. Experimental data are compared with the Dell & Bray model [19] in **Table II** based on two assumptions. In one case, the model is applied assuming that the charge of one calcium atom is equivalent to two sodium atoms; the  $R$  ratio in the model becomes  $R = (\text{Na}_2\text{O} + \text{CaO})/\text{B}_2\text{O}_3$ . In the second case it is postulated that only sodium can compensate the charge of four-coordinate boron, and that all the calcium forms NBOs.

In  $^{17}\text{O-Si}$  glass, 56% of the boron should be found at coordination number 4 if sodium is the only charge compensator. The slightly higher experimental value (60%) indicates that part of the calcium can also be

charge-compensating, although this proportion remains low, as boron charge compensation indiscriminately by either Na or Ca would result in 69% 4-coordinate boron. In complex borosilicate glasses, X-ray absorption spectroscopy has shown that zirconium was at coordination number 6 connected to silicon tetrahedra, with  $[\text{ZrO}_6]^{2-}$  groups requiring compensation by two positive charges [23]. In aluminoborosilicates, the  $[\text{AlO}_4]^-$  groups are generally compensated rather than the  $[\text{BO}_4]^-$  groups, in proportions that depend on the type of network-modifying cation [24]. By assuming that zirconium exhibits the same behavior as aluminum in terms of preferential compensation, we first applied the Dell & Bray model by removing the cations necessary to compensate zirconium ( $R = (\text{Na}_2\text{O} + \text{CaO} - \text{ZrO}_2)/\text{B}_2\text{O}_3$ ). The result largely overestimated the number of four-coordinate boron atoms (65% instead of 44%). If it is assumed that only sodium can be a charge compensator for boron and zirconium, the ratio is consistent with the experimental data. According to this hypothesis, no calcium atoms compensate for zirconium and all the calcium forms NBOs. Similarly, a very significant drop in four-coordinate boron is observed in aluminoborosilicate glass if 20% of the  $\text{K}_2\text{O}$  is replaced by 20%  $\text{CaO}$  [9]. The double charge of calcium certainly makes the system more stable by forming Si-O-Ca-O-Si groups instead of Si-O-Na.

More precise data can be obtained using the  $^{17}\text{O}$  nucleus, which provides a general overview of the structural groups. A  $^{17}\text{O}$  3QMAS spectrum can discriminate between the contributions of different structural groups in simple glasses and qualitatively estimate their relative proportions. A quantitative approach is not directly possible since all the sites are not uniformly excited; the coherence transfer efficiency (central transition multiquantum to single-quantum coherence) of the MQMAS sequence depends mainly on the quadrupolar interaction and radiofrequency field. Taking these effects into account in addition to sample rotation allows the efficiency curve to be determined versus the quadrupolar interaction for a powder sample. It allows to correct the sites intensity if their distribution is low [16]. **Figure 2** shows the relative site excitation profiles versus the quadrupolar coupling constant  $C_Q$  for different values of the asymmetry parameter  $\eta$ .

The glass 3QMAS spectra are shown in **Figure 3a** ( $^{17}\text{O}$ -Si glass) and **Figure 3b** ( $^{17}\text{O}$ -Si-Zr glass). The NMR parameters of the bridging oxygen sites involving silicon and boron (Si-O-Si, Si-O-B and B-O-B) are similar to those previously observed in a sodium aluminoborosilicate glass [11]. Furthermore, the

nonbridging Si-O-Na<sup>+</sup> and Si-O-Ca<sup>2+</sup> sites can be assigned unequivocally. These sites show the predominance of a distribution according to the chemical shift interaction, as recently observed in aluminoborosilicate glass containing potassium or calcium [9]. In SiO<sub>2</sub>-ZrO<sub>2</sub> gels formed by the alkoxide process, the separation between Zr-O-Zr, Si-O-Zr and Si-O-Si sites is clearly visible in the <sup>17</sup>O MAS spectra [25]. The Si-O-Zr site is situated near 150 ppm, similar to the value of the site observed here in the glass containing zirconium. Two-dimensional NMR here reveals this site for the first time, well separated from the others. The data are consistent with X-ray absorption spectroscopy observations of inactive R7T7 glass [23] and confirm the absence of seven-coordinate Zr (ZrO<sub>2</sub>) in sodium-calcium borosilicates.

The following methodology was used to process the MQMAS spectra to extract and quantify the NMR parameters of each site. We initially approached the problem through an inversion procedure [16] to reconstruct the NMR parameter distribution numerically for each of the MQMAS spectrum sites. This type of reconstruction allows us to quickly determine the mean NMR parameter values for each site. For quantification purposes, these distributions could then be fitted with analytical models. However, we chose to fit the MQMAS spectra directly using analytical distribution models also taking into account the effects of excitation of the MQMAS sequence (see **Figure 2**). For the distribution model we chose the product of three Gaussians, one for each NMR parameter (no correlation between the parameters taken into account underway and should be presented elsewhere), i.e. the quadrupolar coupling constant  $C_Q$ , the quadrupolar asymmetry parameter  $\eta$  and the isotropic chemical shift  $\delta_{iso}$ . We obtained the simulated spectrum in **Figure 3d**, in close agreement with the experimental spectrum. To the best of our knowledge, this is the first attempt to a direct quantitative simulation of the <sup>17</sup>O MQMAS spectra. This type of approach allows direct quantification of the MQMAS spectrum. The NMR parameter set obtained for <sup>17</sup>O-Si glass was unmodified to quantify the spectrum of <sup>17</sup>O-Si-Zr glass (and was found to yield satisfactory results). The same parameter set can be used to fit the MAS spectrum. We had to adopt this approach to quantify the relative proportion of Si-O-Zr compared with the other sites because this was not possible using the MQMAS spectrum due to experimental limitations (insufficient rotation speed resulting in MQMAS spectrum distortions near the Si-O-Zr site). The mean NMR parameter values of each site are indicated in



**Table III.** The broad distribution of the Si-O-Zr site made it impossible to determine the asymmetry parameter  $\eta$ .

Du and Stebbins [9] proposed two approaches for theoretically computing the proportions of various groups from the chemical composition of aluminoborosilicates. A random distribution of the groups in the glass structure is assumed or, conversely, some groups are considered unable to form. We adapted these models to our compositions; the fact that bonds are prohibited between four-coordinate elements (except for silicon) was extended to bonds between octahedral zirconium and four- or six-coordinate groups (except for Si). With these hypotheses the following groups are prohibited:  ${}^4\text{B-O-}{}^4\text{B}$ ,  ${}^6\text{Zr-O-}{}^6\text{Zr}$ , and  ${}^6\text{Zr-O-}{}^4\text{B}$ . We assume all the zirconium is in octahedral form. The proportion of four-coordinate boron taken into account was the value measured by  ${}^{11}\text{B}$  NMR. The results are indicated in **Table IV**.

The random distribution model provides a better fit, although the differences with the experimental data are still significant. The Si-O-B bonds are overestimated by the models in both glasses, whereas the B-O-B bonds are underestimated for  ${}^{17}\text{O}$ -Si glass. For the latter glass, the result lies between the description proposed by Dell & Bray [19], in which borate and silicate subnetworks are discriminated, and a purely random distribution of the groups. Conversely, the boron distribution in  ${}^{17}\text{O}$ -Si-Zr glass is very near a random distribution with regard to the B-O-B bonds. Zirconium could account for the disappearance of the borate subnetwork following the formation of B-O-Zr bonds. Under these conditions, no distinction could be made in the  ${}^{17}\text{O}$  MQMAS spectra between Si-O-Zr and B-O-Zr groups. This hypothesis is supported by the proportions obtained by NMR (**Table III**): the Si-O-Si sites are found in large amounts whereas bonds involving boron are present only in small numbers. In other words, the formation of B-O-Zr bonds leaves more Si available for the formation of Si-O-Si sites and less B available to form B-O-B and Si-O-B bonds. This could also account for the broad distribution of this site over the MQMAS spectrum, which could be related to the presence of both Si-O-Zr and B-O-Zr. In the same way, it has been suggested that adding aluminum to a borosilicate glass could lead to a drop in phase separations with the formation of B-O-Al-O-Si units [22]. Zirconium could exhibit behavior similar to that of aluminum.

The nonbridging sites are largely underestimated by the calculation—in particular for glass containing no Zr, for which the NBO fraction is lower by a factor of four. NBOs arise mainly from calcium atoms (three

to five times more numerous than sodium-bonded NBOs). The excess NBO fraction has already been observed experimentally in aluminosilicate [26] and borosilicate [27] glass compositions and attributed to the presence of oxygen triclusters compensating the NBOs. These observations were confirmed by ab initio molecular dynamics calculations [28,29]. The quadrupolar coupling constant that could be assigned to this type of site (about 2.3–2.6 MHz) would make it relatively difficult to observe here due to the proximity with nonbridging sites. Nonbridging sites could also be found with tricoordinate boron and be indistinguishable on the MQMAS spectrum with bridging oxygen bonded to silicon [4].

### 3.2 Gel structure

The glass compositions used for the leaching experiments differed slightly from those of the two glasses enriched in oxygen-17 characterized in the preceding section. To obtain a sufficient quantity of gel to ensure a useful NMR signal, we increased the quantity of soluble elements—sodium in this case. **Table V** gives the molar compositions of the pristine glass samples and of the resulting alteration gels (inferred from the boron released into solution as an alteration tracer). The element retention factors in the gel are indicated in the right-hand side of the **Table V**.

In the gel of the glass containing no Zr ( $^{17}\text{O}$ -Si gel), the only remaining elements were silicon and calcium. The greater Ca retention in the gel shows that part of the Si is released in the solution. The quantity of altered glass was only half that of the glass initially containing zirconium. In that later case ( $^{17}\text{O}$ -Si-Zr gel), the Si retention rate exceeded 90%; the Zr atoms appeared to let Si atoms less soluble. These highly insoluble and rigid “hard” nuclei could also make silica recondensation more difficult and thus enhance preferential exchange pathways between the glass and the leaching solution [12]. This mechanism could account for the large quantity of gel observed on the glass containing Zr. Equilibrium with solution—particularly with Si—was delayed and the glass continued to be altered. This gel also contained cations in same proportions as Zr, with about 20% Na and 80% Ca. The  $^{11}\text{B}$  spectra of the pristine glass were more consistent with the model if sodium was assumed to compensate both boron and zirconium. This appears to be in contradiction with 80% Ca compensation in the gel, unless rearrangements occurred during leaching and exchanges between charge compensators occurred near Zr. This type of mechanism has already been observed in alteration gels around aluminum with the substitution of Ca for the Na

compensating  $[\text{AlO}_4]^-$  during leaching [2]. This would imply compensation of zirconium mainly by sodium in the pristine glass and by calcium in the gel.

The  $^{17}\text{O}$  3QMAS spectrum of this gel is relatively noisy (**Figure 4**) but nevertheless reveals a Si-O-Zr site of the same type as earlier observed in glass, but with a more limited distribution. The structural configuration of Zr would then sustain little or no change during leaching, and the  $[\text{ZrO}_6]^{2-}$  groups would be conserved. If the coordination number is conserved, NBOs could certainly be found around Zr due to the release of boron if B-O-Zr bonds are postulated. The sites present in the gel (**Table VI**) were quantified directly from the MAS spectra, as the small quantity of gel resulted in poor resolution of the 3QMAS spectra (**Figure 4**). The presence of Ca was nevertheless observed in the gel containing no Zr. Nonbridging sites were not detectable in  $^{17}\text{O}$ -Si-Zr gel, but appear to be present in the MAS spectrum. It is relatively surprising to find 6% NBO in the gel containing Zr insofar as Ca should be a Zr charge compensator. This site is nevertheless not found at the same position as in the pristine glass, but is displaced toward higher chemical shifts and could correspond to charge-compensating Ca. This could imply a different configuration than that of the glass, which is due to the presence of NBOs around Zr. Nearby calcium atoms could then contribute to the NMR signal observed here. The proportion of Si-O-Zr sites is fully consistent with the solutions analysis findings if the molar proportions in the gel are compared with the number of Zr-O-Si bonds. In the same way, the proportions of Si-O-Ca sites in the  $^{17}\text{O}$ -Si gel are also consistent.

#### 4. Conclusion

A method of quantitative analysis of the  $^{17}\text{O}$  MQMAS spectra is presented, by fitting directly the two-dimensional MQMAS spectrum which provides the resolution of all the structural groups forming the glass network. Additional data for this analysis are also obtained from the quantitative deconvolution of the  $^{11}\text{B}$  MAS NMR spectra. Alteration layers arising from glass leaching were also probed by oxygen-17 supplied by the leaching solution. Preferential compensation mechanisms of sodium with respect to boron and zirconium rather than calcium in the glass are proposed. Although most of the zirconium is inserted in the silicate network forming Si-O-Zr bonds, the presence of this element tends to reduce the extent of a

borate subnetwork by forming B-O-Zr bonds. Excess nonbridging oxygen is clearly identified in the glasses, and could be related to the presence of oxygen triclusters. During leaching, calcium clearly remains in the alteration gel, either stabilized near nonbridging oxygens or as a zirconium charge compensator, as zirconium conserves the same coordination number in the glass. Zirconium increases the rigidity of the glass structure, but by making silicon dissolution and reprecipitation more difficult, it results in larger quantities of altered glass. This quantitative approach of  $^{17}\text{O}$  MQMAS spectra by an inversion method taking into account the MQMAS sequence excitation effects thus demonstrates its potential for investigating the structure of increasingly complex glass compositions.

## 5. References

- [1] Gin S., *Mat. Res. Soc. Symp. Proc.* XXIV 663, 207–215 (2000)
- [2] Angeli F., Gaillard M., Jollivet P., Charpentier T., *Geochim. Cosmochim. Acta* 70 (2006) 2577–2590
- [3] Frydman L., Harwood J.S., *J. Am. Chem. Soc.*, 117, 5367 (1995)
- [4] Stebbins J.F., Zhao P., Kroeker, *Solid State Nuclear Magnetic Resonance* 16, 9–19 (2000)
- [5] Lee S.K., Stebbins J.F., *J. Phys. Chem. B*, 104 (17), 4091–4100 (2000)
- [6] Stebbins, J.F., Oglesby J.V., Lee S.K., *Chem. Geol.* 174, 63–75 (2001)
- [7] Du L.S., Stebbins J.F., *Chem. Mater.* 15, 3913–3921 (2003)
- [8] Du L.S., Stebbins J.F., *Solid State Nuclear Magnetic Resonance*, 27, 37–49 (2005)
- [9] Du L.S., Stebbins J.F., *J. Non-Cryst. Solids*, 351, 3508–3520 (2005)
- [10] Lee S.K., Cody G.D., Fei Y.W., Mysen B.O., *Chemical geology* 229 (1–3): 162–172 (2006)
- [11] Angeli F., Charpentier T., Gin S., Petit J.C., *Phys. Chem. Lett.* 341 (2001) 23.
- [12] Arab M., Cailleateau C., Angeli F., Devreux F., Girard L., Spalla O., *J. Non-Cryst. Solids*, submitted
- [13] Massiot D., Bessada C., Coutures J.P., Virlet J., Tautelle F., *J. Magn. Reson.*, 90, 231 (1990)
- [14] Fernandez C., Amoureux J.P., *Chem. Phys. Lett.*, 242, 449 (1995)
- [15] Charpentier T., Fermon C., Virlet J., *J. Chem. Phys.*, 109, 3116 (1998)
- [16] Angeli F., Charpentier T., Faucon P., Petit J.C., *J. Phys. Chem. B*, 103, 10356 (1999)
- [17] Yun Y.H., Bray P.J., *J. Non-Cryst. Solids*, 27, 363 (1978)
- [18] Xiao S.Z., *J. Non-Cryst. Solids*, 45, 29 (1981)
- [19] Dell W., Bray P.J., Xiao S.Z., *J. Non-Cryst. Solids*, 58, 1 (1983)
- [20] Yamashita H., Yoshino H., Nagata K., Inoue H., Nakajin T., Maekawa T., *J. Non-Cryst. Solids*, 270 (1–3) (2000)
- [21] Yamashita H., Inoue K., Nakajin T., Inoue H., Maekawa T., *J. Non-Cryst. Solids*, 331 (128–136) (2003)
- [22] Du W.F., Kuraoka K., Akai T., Yazawa T., *J. Mater. Science* 35(19) (2000) 4865–4871
- [23] Galois L., Pelegrin E., Arrio M.A., Ildefonse P. and Calas G. (1999), *J. Am. Ceram. Soc.* 82(8), 2219–2224

- [24] Chan J.C.C., Bertmer M., Eckert H., *J. Am. Chem. Soc.* 121 (1999) 5238–5248
- [25] Dirken P.J., Dupree R., Smith M.E., *Mat. Chem. Comm.* 5(8) (1995), 1261–1263
- [26] Stebbins J.F., Xu Z., *Nature* 390 (1997), 60–62
- [27] Zhao P., Kroeker S., Stebbins J.F., *J. Non-Cryst. Solids*, 276, 122–131 (2000)
- [28] Tossel J.A., Horbach J., *J. Phys. Chem. B*, 109, 1794–1797 (2005)
- [29] Benoit M., Profeta M., Mauri F., Pickard C.J., Tuckerman M.E., *J. Phys. Chem. B*, 109, 6052–6060 (2005)

**Table I.** Molar composition of glass enriched in oxygen-17

	SiO <sub>2</sub> (mol%)	B <sub>2</sub> O <sub>3</sub> (mol%)	Na <sub>2</sub> O (mol%)	CaO (mol%)	ZrO <sub>2</sub> (mol%)
<sup>17</sup> O-Si glass	70.0	17.8	9.9	2.3	–
<sup>17</sup> O-Si-Zr glass	67.2	15.5	10.4	3.3	3.6

**Table II.** NMR parameters obtained for simulations of <sup>11</sup>B MAS peaks and comparison of site quantification with variants of the Dell & Bray model

Glass	Site	$\delta_{iso}$ (ppm)	$C_Q$ (MHz)	$\eta$	Relative intensity	D&B Model Na <sub>2</sub> O=CaO	D&B Model Ca-B avoidance
<sup>17</sup> O-Si glass	BO <sub>3s</sub>	18.3	2.5	0.1	22	31	44
	BO <sub>3a</sub>	14.0	2.8	0.3	18		
	BO <sub>4</sub>	0.2	0.3	0	60		
<sup>17</sup> O-Si-Zr glass	BO <sub>3s</sub>	18.8	2.5	0	31	35	56
	BO <sub>3a</sub>	14.0	2.8	0.2	25		
	BO <sub>4</sub>	0.3	0.2	0	44		

**Table III.** NMR parameters and quantification of different <sup>17</sup>O sites

Glass	Sites	$\delta_{iso}$ (ppm)	$C_Q$ (MHz)	$\eta$	Proportion (%)
<sup>17</sup> O-Si glass	Si-O-Si	51.9	4.9	0.4	43.7
	Si-O-B	65.2	5.3	0.4	34.6
	B-O-B	86.8	5.0	0.2	15.5
	Si-O-Na	38.9	2.5	0.3	1.2
	Si-O-Ca	74.2	2.8	0.4	5.0
<sup>17</sup> O-Si-Zr glass	Si-O-Si	51.9	4.9	0.4	53.2
	Si-O-Zr	126.3	3.0	–	12.8
	Si-O-B	65.2	5.3	0.4	23.6
	B-O-B	86.8	5.0	0.2	6.3
	Si-O-Na	38.9	2.5	0.3	1.0
	Si-O-Ca	74.2	2.8	0.4	3.1

**Table IV.** Proportions of different sites computed from a random distribution model and a model prohibiting certain bonds (refer to text)

Glass	Si-O-B	Si-O-Zr	Zr-O-B	Si-O-Si	B-O-B	Zr-O-Zr	NBO
<sup>17</sup> O-Si glass Random mixing	42.6	–	–	46.0	9.9	–	1.5
<sup>17</sup> O-Si-Zr glass Random mixing	35.5	7.2	2.9	43.6	7.2	0.3	3.3
<sup>17</sup> O-Si glass Non-random mixing	49.2	–	–	42.8	6.6	–	1.5
<sup>17</sup> O-Si-Zr glass Non-random mixing	38.9	8.9	1.8	41.1	6.1	–	3.3

**Table V.** Molar composition of pristine glass and alteration gels inferred from solution analysis after approximately 6 months of leaching in pure water. The altered glass percentage is indicated in the column headed "Gel %". The right-hand part of the table indicates the element retention factors in the gel (compared with boron)

	Composition (mol%)						Retention factor (%)			
	SiO <sub>2</sub>	B <sub>2</sub> O <sub>3</sub>	Na <sub>2</sub> O	CaO	ZrO <sub>2</sub>	Gel %	Si	Zr	Ca	Na
O-Si glass	61.4	16.9	18.1	3.6						
O-Si-Zr glass	56.5	17.5	18.3	3.8	3.9					
<sup>17</sup> O-Si gel	92.5			7.5		2.6	71	–	97	–
<sup>17</sup> O-Si-Zr gel	86.8		1.6	5.1	6.6	5.1	91	100	79	5

**Table VI.** Quantification of groups present within the alteration gels

Glass	Si-O-Si	Si-O-Ca	Si-O-Zr
Si gel	92	8	–
Si-Zr gel	73.5	6	20.5

## FIGURES

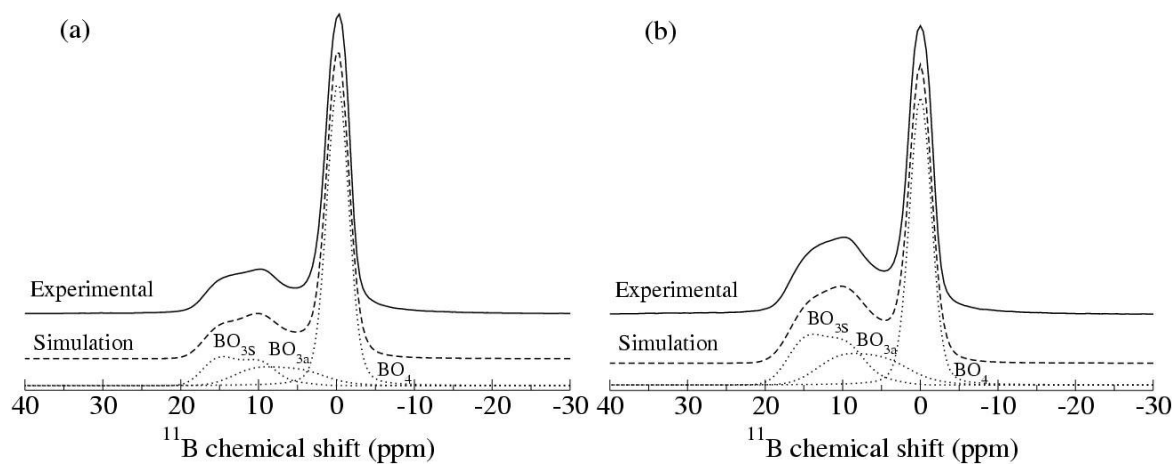


**Figure 1.**  $^{11}\text{B}$  MAS spectra and deconvolution of glass enriched in oxygen-17 without zirconium (a) and with zirconium (b)

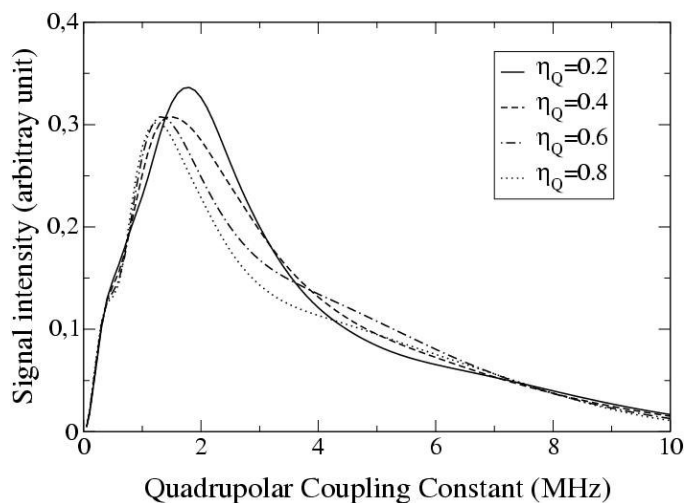


**Figure 2.** Excitation profiles versus quadrupolar coupling constant for the 3QMAS sequence (spin  $I = 5/2$ ) used in this study with different values of the asymmetry parameter  $\eta$  (rotation speed: 14 kHz)



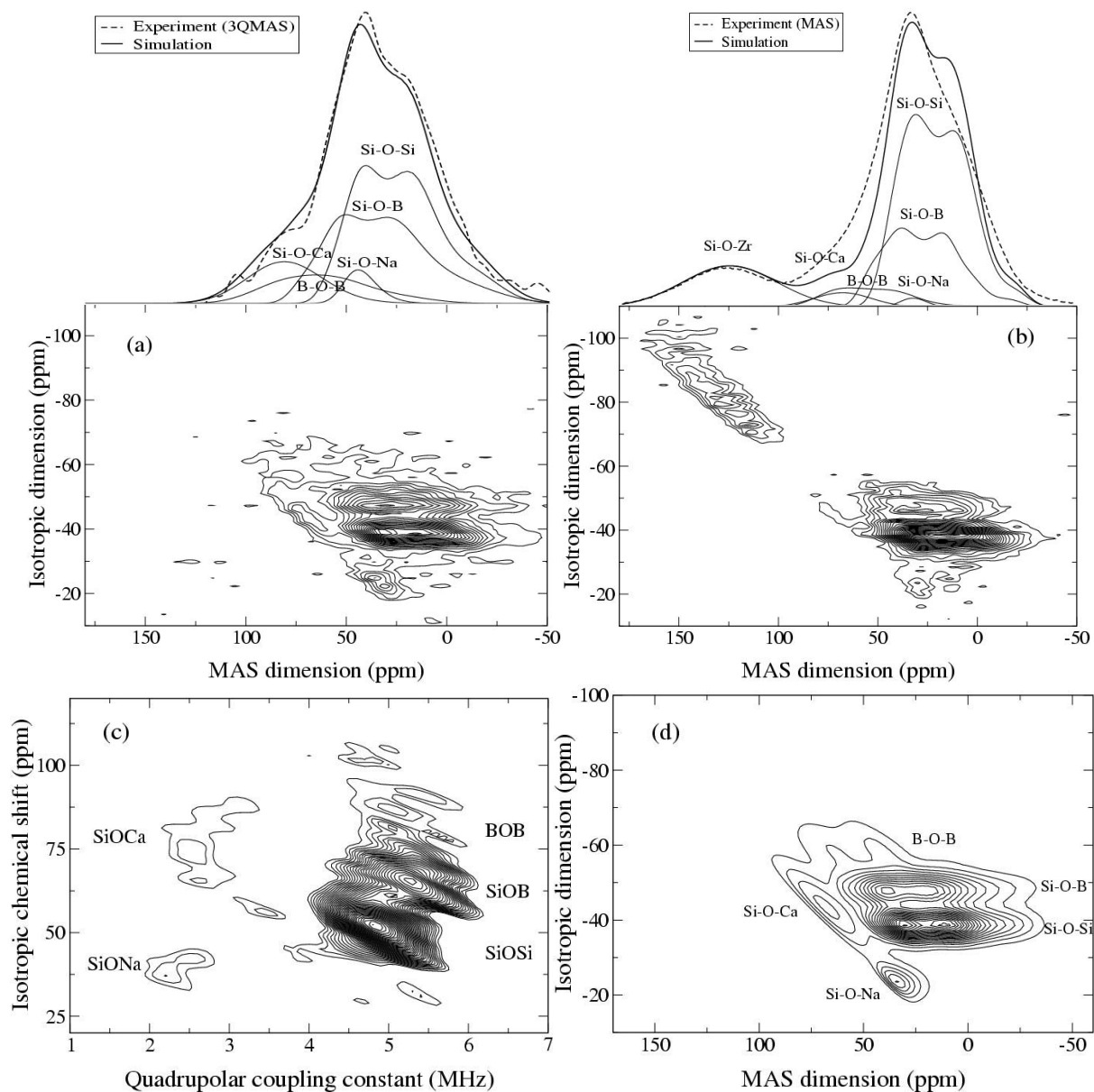


**Figure 3.**  $^{17}\text{O}$  3QMAS spectra of  $70\text{SiO}_2-17.8\text{B}_2\text{O}_3-9.9\text{Na}_2\text{O}-2.3\text{CaO}$  glass (a) and  $67.2\text{SiO}_2-15.5\text{B}_2\text{O}_3-10.4\text{Na}_2\text{O}-3.3\text{CaO}-3.6\text{ZrO}_2$  glass (b); (c) represents the  $\delta_{iso}$  and  $C_Q$  distributions of the first glass obtained after inversion of the 3QMAS spectra; (d) represents the simulated 3QMAS spectrum.

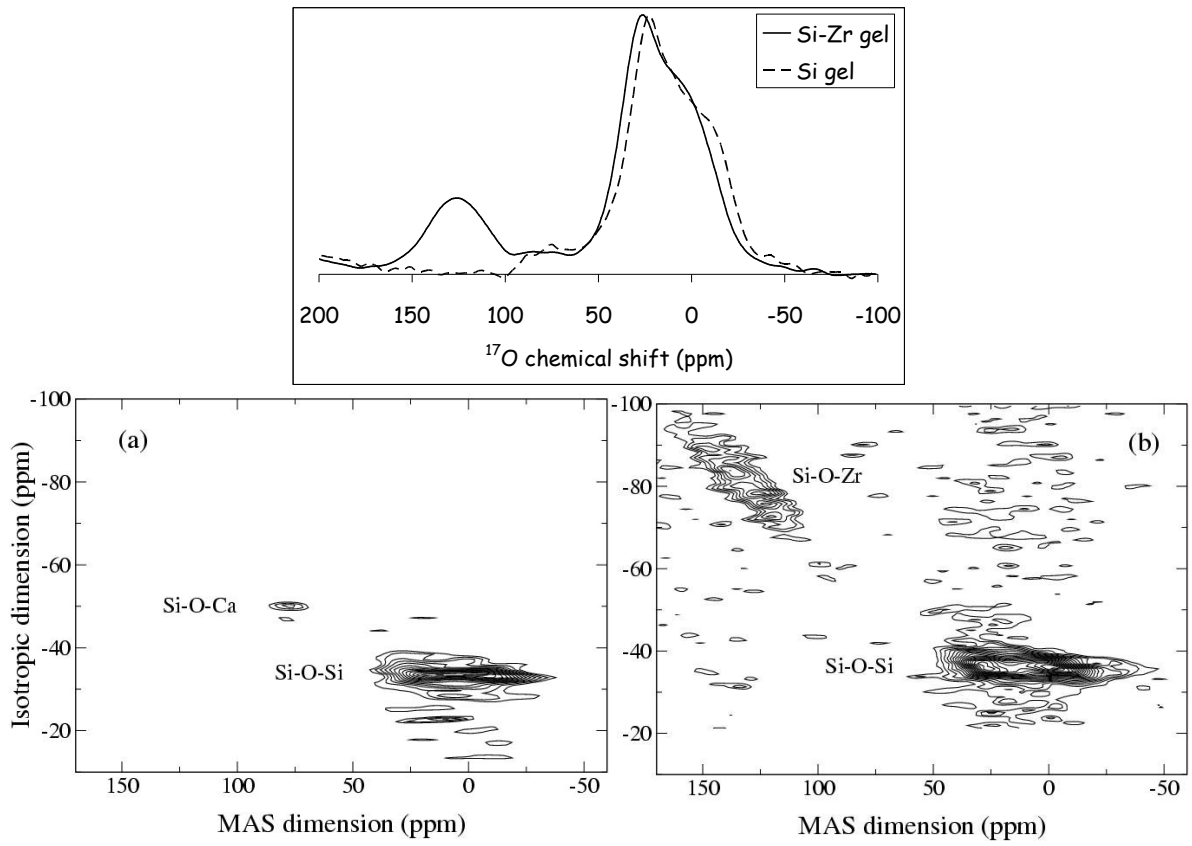


**Figure 4.**  $^{17}\text{O}$  MAS (top) and 3QMAS (bottom) spectra of  $^{17}\text{O}$ -Si gel (a) and  $^{17}\text{O}$ -Si-Zr gel (b)